PHYSICAL REVIEW D **80,** 045006 (2009)

Universal constraints on conformal operator dimensions

Vyacheslav S. Rychkov[1] and Alessandro Vichi[2]
[1]*Scuola Normale Superiore and INFN, 56100 Pisa, Italy*
[2] *Institut de Théorie des Phénomènes Physiques, EPFL, 1015 Lausanne, Switzerland*
(Received 11 June 2009; published 7 August 2009)

We continue the study of model-independent constraints on the unitary conformal field theories (CFTs) in four dimensions, initiated in [R. Rattazzi, V. S. Rychkov, E. Tonni, and A. Vichi, J. High Energy Phys. 12 (2008) 031]. Our main result is an improved upper bound on the dimension Δ of the leading scalar operator appearing in the operator product expansion (OPE) of two identical scalars of dimension d: $\phi_d \times \phi_d = \mathbb{1} + O_\Delta + \ldots$. In the interval $1 < d < 1.7$ this universal bound takes the form $\Delta \leq 2 + 0.7(d-1)^{1/2} + 2.1(d-1) + 0.43(d-1)^{3/2}$. The proof is based on prime principles of CFT: unitarity, crossing symmetry, OPE, and conformal block decomposition. We also discuss possible applications to particle phenomenology and, via a 2D analogue, to string theory.

DOI: 10.1103/PhysRevD.80.045006 PACS numbers: 11.15.Tk, 11.25.Hf, 14.80.−j

I. INTRODUCTION AND FORMULATION OF THE PROBLEM

Our knowledge about nonsupersymmetric conformal field theories (CFTs) in four dimensions is still quite incomplete. Suffice it to say that not a single nontrivial example is known which would be solvable to the same extent as, say, the 2D Ising model. However, we do not doubt that CFTs must be ubiquitous. For example, nonsupersymmetric gauge theories with N_c colors and N_f flavors are widely believed to have "conformal windows" in which the theory has a conformal fixed point in the IR, with evidence from large N_c analysis [1], supersymmetric analogues [2], and lattice simulations [3]. Since these fixed points are typically strongly coupled, we do not have much control over them. In this situation particularly important are general, model-independent properties.

One example of such a property is the famous unitarity bound [4] on the dimension Δ of a spin l conformal primary operator $O_{\Delta,l}$[1]:

$$\Delta \geq 1 \quad (l = 0), \qquad \Delta \geq l + 2 \quad (l \geq 1). \tag{1.1}$$

These bounds are derived by imposing that the two-point functions $\langle OO \rangle$ have a positive spectral density.

As is well known, three-point functions in CFT are fixed by conformal symmetry up to a few arbitrary constants [operator product expansion (OPE) coefficients]. The next nontrivial constraint thus appears at the four-point function level, and is known as the *conformal bootstrap* equation. It says that OPE applied in the direct and crossed channel should give the same result (see Fig. 1).

The bootstrap equation goes back to the early days of CFT [5]. However, until recently, not much useful general information has been extracted from it.[2] All spins and dimensions can *a priori* enter the bootstrap on equal footing, and this seems to lead to unsurmountable difficulties.

Recently, however, tangible progress in the analysis of bootstrap equations was achieved in [7]. Namely, it was found that, in unitary theories, the functions entering the bootstrap equations (conformal blocks) satisfy certain *positivity properties* which lead to general necessary conditions for the existence of solutions.

The concrete problem considered in [7], and which we will continue to discuss here, was as follows. In an arbitrary unitary CFT a Hermitian scalar primary ϕ_d of dimension d was singled out. The conformal bootstrap equation for its four-point function $\langle \phi_d \phi_d \phi_d \phi_d \rangle$ was studied under the sole assumption that all *scalars* in the OPE $\phi_d \times \phi_d$ have dimension above a certain number, call it $\Delta_{\min}$:

$$\phi_d \times \phi_d = \mathbb{1}(\text{Scalars of dimensions} \geq \Delta_{\min}) + (\text{Higher spins}). \tag{1.2}$$

It was shown that the conformal bootstrap *does not allow for a solution* unless

$$\Delta_{\min} \leq f(d), \tag{1.3}$$

where $f(d)$ is a certain continuous function, computed numerically. We stress that this conclusion was reached without making any assumptions about dimensions or spins of other operators appearing in the OPE, beyond those implied by the unitarity bounds. Nor any assump-

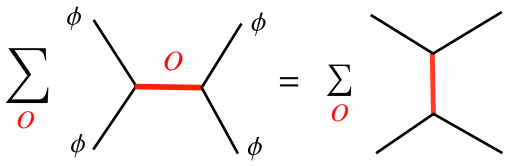

FIG. 1 (color online). The conformal bootstrap equation. The red (dark gray) line denotes a conformal block, summing up exchanges of a primary operator O and all its descendants.

[1]Here we quote only the case of symmetric traceless tensor operators.

[2]Except in 2D, in theories with finitely many primary fields, and in the Liouville theory [6]. We will comment on the 2D case in Secs. IVA and V below.

tions about the OPE coefficients were made (apart from their reality, which is again implied by unitarity).

In other words, *in any unitary 4D CFT, the OPE of any scalar primary ϕ_d must contain at least one scalar field O_Δ with dimension not larger than $f(d)$.*

Incidentally, the function $f(d)$ was found to satisfy $f(1) = 2$, which is quite natural since $d = 1$ corresponds to the free field whose OPE contains the operator $:\phi^2:$ of dimension 2.

What makes the result like (1.3) possible? The basic reason is that, in any theory, the crossing symmetry relation of Fig. 1 cannot be satisfied term by term, but only by cancellations among various terms. The guaranteed presence of the unit operator in the OPE (1.2) creates a certain "crossing symmetry deficit," which has to be balanced by other fields. The idea is to show that this cannot happen unless at least one scalar of sufficiently low dimension is present.

Technically, the method of [7] consists of 3 steps (see Sec. III for a detailed review):

(1) We Taylor-expand the conformal bootstrap equation near the "self-dual point" configuration having equal conformal cross-ratios $u = v$. The expansion is truncated to a certain finite order N.
(2) We systematically search for *positivity properties* satisfied by linear combinations of Taylor coefficients of the conformal blocks, for fields appearing in the right-hand side (RHS) of the OPE (1.2). A found positivity property implies that the "crossing symmetry deficit" cannot be balanced and rules out a CFT with a given d and $\Delta_{\min}$.
(3) For fixed d, the bound $f(d)$ is then computed as the point separating those $\Delta_{\min}$ for which a positivity property exists, from those ones for which it does not (Fig. 2).

The nature of the method is such that increasing N can make the bound only stronger. The optimal bound should in principle be recoverable in the limit $N \to \infty$. In practice the value of N is determined by the available computer resources and algorithmic efficiency. The best bound found in [7], plotted in Fig. 3, corresponds to $N = 6$.

The purpose of this paper is to present an improvement of the bound (1.3) obtained by using the method of [7] with larger values of N, up to $N = 18$. The new results are interesting in two ways. First, pure numerical improvement turns out to be significant. Second, $N = 18$ happens to be large enough so that we start observing saturation of the bound. So we believe our current results are close to the optimal ones achievable with this method.

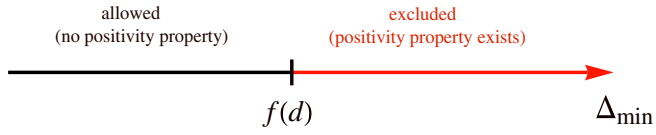

FIG. 2 (color online). The bound $f(d)$ is the smallest $\Delta_{\min}$ for which a positivity property exists.

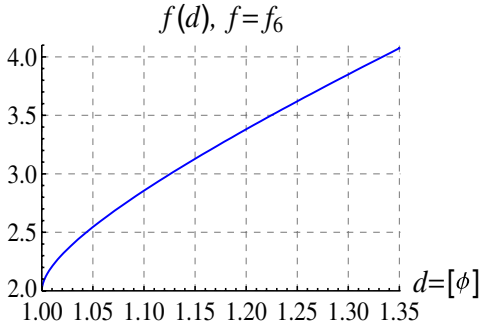

FIG. 3 (color online). The bound $f_6(d) \simeq 2 + 1.79\sqrt{d-1} + 2.9(d-1)$, $1 \le d \le 1.35$, corresponding to $N = 6$, reproduced from [7].

The paper is organized as follows. In Sec. II we review the conformal bootstrap equations. In Sec. III we review the connection of the bound (1.3) with positivity properties satisfied by the conformal block expansion coefficients. In Sec. IV we present and discuss our results. We also mention accompanying results which we obtain for an analogous problem in 2D. In Sec. V we propose several future applications and extensions of our method, with emphasis on connections to phenomenology and string theory. In Sec. VI we summarize and conclude. In Appendix A we collect some details about our numerical algorithms. In Appendix B we include the tables on which plots in Sec. IV are based.

II. REVIEW OF CONFORMAL BOOTSTRAP

We will review the conformal bootstrap equation in its simplest form—as applied to the four-point function of identical scalars $\langle\phi\phi\phi\phi\rangle$. We largely follow [7], where a more detailed discussion and references can be found.

A. Conformal block decomposition

Let $\phi \equiv \phi_d$ be a Hermitian scalar primary[3] operator. The OPE $\phi \times \phi$ contains, in general, infinitely many primary fields of arbitrary high spins and dimensions[4]:

$$\phi(x)\phi(0) \sim \frac{1}{|x|^{2d}}\left\{\mathbb{1} + \sum_{l=2n} c_{\Delta,l}[|x|^{-\Delta}K_l(x)\cdot O_{\Delta,l}(0) + \cdots]\right\},$$
$$K_l(x) = \frac{x^{\mu_1}\cdots x^{\mu_l}}{|x|^l}. \tag{2.1}$$

Here

(i) $l = 2n$ by Bose symmetry;

[3]The field is called primary if it transforms homogeneously under the 4D conformal group.

[4]If there are several primaries with the same Δ, l, they all have to be included in this sum with independent coefficients.

(ii) $\Delta \geq 1$ ($\Delta \geq l+2$) for $l=0$ ($l \geq 2$) by the unitarity bounds (1.1);
(iii) The ... stands for contributions of descendants of the primary $O_{\Delta,l}$ (i.e. its derivatives). These contributions are fixed by conformal symmetry;
(iv) The OPE coefficients $c_{\Delta,l}$ are real (see Appendix A of [7]).

We assume that the OPE converges in the following weak sense: it gives a convergent power series expansion for any $(2+n)$-point function

$$\langle \phi(x)\phi(0)A_1(y_1)\dots A_n(y_n)\rangle$$

provided that $|x|<|y_i|$, i.e. $\phi(x)$ is closer to the origin than any other local field insertion (see Fig. 4). This assumption can be justified by using radial quantization ([8], Sect. 2.9), and checked explicitly in free field theory. For rigorous mathematical results about OPE convergence, see [9].

The OPE (2.1) can be used to obtain *conformal block decomposition* of the four-point function $\langle\phi\phi\phi\phi\rangle$:

$$\langle \phi(x_1)\phi(x_2)\phi(x_3)\phi(x_4)\rangle = \frac{g(u,v)}{x_{12}^{2d}x_{34}^{2d}}, \tag{2.2}$$

$$g(u,v) = 1 + \sum p_{\Delta,l} g_{\Delta,l}(u,v), \qquad p_{\Delta,l} \equiv c_{\Delta,l}^2 \geq 0, \tag{2.3}$$

where $u = x_{12}^2x_{34}^2/(x_{13}^2x_{24}^2)$, $v = x_{14}^2x_{23}^2/(x_{13}^2x_{24}^2)$ are the conformal cross-ratios. This representation is obtained by using the OPE in the 12 and 34 channels. The *conformal blocks* $g_{\Delta,l}(u,v)$ sum up the contributions of the primary $O_{\Delta,l}$ and all its descendants. Their explicit expressions were found by Dolan and Osborn [10]:

$$\begin{aligned} g_{\Delta,l}(u,v) &= \frac{(-)^l}{2^l}\frac{z\bar z}{z-\bar z}[k_{\Delta+l}(z)k_{\Delta-l-2}(\bar z) - (z\leftrightarrow\bar z)], \\ k_\beta(x) &\equiv x^{\beta/2}{}_2F_1(\beta/2,\beta/2,\beta;x), \\ u &= z\bar z, \qquad v = (1-z)(1-\bar z). \end{aligned} \tag{2.4}$$

Notice the judicious introduction of the auxiliary variables z and $\bar z$. When the theory is formulated in the Euclidean space, these variables are complex conjugates of each other. To understand their meaning, it is convenient to use the conformal group freedom to send $x_4 \to \infty$ and to put the other three points in a plane, as in Fig. 5. Then it's

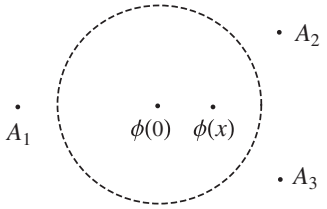

FIG. 4. The operator product expansion of $\phi(x)\phi(0)$ converges for this configuration.

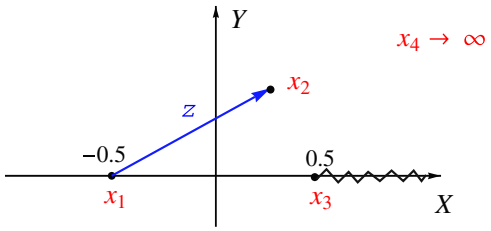

FIG. 5 (color online). The auxiliary z coordinate. The conformal blocks are regular outside the cut denoted by the zigzag line.

easy to show that

$$z = \frac{1}{2} + X + iY, \qquad \bar z = z^*, \tag{2.5}$$

where (X, Y) are the coordinates of x_2 in the plane, chosen so that $X=Y=0$ corresponds to x_2 halfway between x_1 and x_3. This "self-dual" configuration, for which $u=v$, will play an important role below. We can see that the z variable is a natural extension of the usual complex coordinate of the 2D CFT to the 4D case.

According to the above discussion, the OPE is expected to converge for $|z|<1$. Conformal block decomposition is a partial resummation of the OPE and thus also converges at least in this range. In fact, below we will only use convergence around the self-dual point $z=1/2$. However, conformal blocks, as given by (2.4), are regular (real-analytic) in a larger region, namely, in the z plane with the $(1,+\infty)$ cut along the real axis (see Fig. 5). The conformal block decomposition is thus expected to converge in this larger region. One can check that this indeed happens in the free scalar theory.

One can intuitively understand the reason for this extended region of regularity. The condition for the OPE convergence, as stated above, does not treat the points x and 0 symmetrically. On the other hand, the conformal blocks are completely symmetric in $x_1 \leftrightarrow x_2$ and so must be the condition for their regularity. The appropriate condition is as follows: *the conformal block decomposition in the* 12–34 *channel is regular and convergent if there is a sphere separating the points* $x_{1,2}$ *from the points* $x_{3,4}$. For the configuration of Fig. 5, such a sphere exists as long as x_2 is away from the cut.

B. Conformal bootstrap and the sum rule

The four-point function in (2.2) must be symmetric under the interchange of any two x_i, and its conformal block decomposition (2.3) has to respect this symmetry. The symmetry with respect to $x_1 \leftrightarrow x_2$ or $x_3 \leftrightarrow x_4$ is already built in, since only even spins are exchanged [10]. On the contrary, the symmetry with respect to $x_1 \leftrightarrow x_3$ gives a condition

$$v^d g(u,v) = u^d g(v,u), \tag{2.6}$$

which is not automatically satisfied for $g(u,v)$ given by

(2.3). This nontrivial constraint on dimensions, spins, and OPE coefficients of all operators appearing in the OPE $\phi \times \phi$ is known as the *conformal bootstrap equation*. Physically it means that OPE applied in 12–34 and 14–23 channels should give the same result (Fig. 1).

In the z plane of Sec. II A, the left-hand side (LHS) of (2.6) has a cut along $(1, +\infty)$, while the RHS has a cut along $(-\infty, 0)$. Thus, if (2.6) is satisfied, the cuts have to cancel, and the resulting $g(u, v)$ is real analytic everywhere except for $z = 0, 1$.

In [7], we found it useful to rewrite (2.6) by separating the unit operator contribution, which gives

$$u^d - v^d = \sum p_{\Delta,l}[v^d g_{\Delta,l}(u, v) - u^d g_{\Delta,l}(v, u)]. \quad (2.7)$$

The LHS of this equation is the "crossing symmetry deficit" created by the presence of the unit operator in the OPE. This deficit has to be balanced by contributions of the other fields in the RHS.

In practice it is convenient to normalize (2.7) by dividing both sides by $u^d - v^d$. The resulting *sum rule* takes the form:

$$1 = \sum p_{\Delta,l} F_{d,\Delta,l}(X, Y),$$
$$F_{d,\Delta,l}(X, Y) \equiv \frac{v^d g_{\Delta,l}(u, v) - u^d g_{\Delta,l}(v, u)}{u^d - v^d}. \quad (2.8)$$

The "F functions" $F_{d,\Delta,l}$ are real and regular in the full z-plane cut along $(-\infty, 0) \cup (1, +\infty)$. In particular, the $0/0$ behavior at the self-dual point $z = 1/2$ is regular.

All F functions vanish near the points $z = 0$ and $z = 1$. Thus the sum rule can never be satisfied near these points if only finitely many terms are present in the RHS. *The OPEs containing finitely many primaries are ruled out.*

III. POSITIVITY ARGUMENT

The main idea of [7] was very simple, and can be described as follows. Suppose that for a given spectrum of operator dimensions and spins $\{\Delta, l\}$ the sum rule (2.8), viewed as an equation for the coefficients $p_{\Delta,l} \geq 0$, has no solution. Then of course such a spectrum would be ruled out.

Any concrete realization of this idea needs a practical criterium to show that there is no solution. For a prototypical example of such a criterium, imagine that a certain derivative, e.g. ∂_X [see (2.5)], when applied to every $F_{d,\Delta,l}$ and evaluated at a certain point, is strictly positive ("positivity property"). Since the same derivative applied to the LHS of (2.8) gives identically zero, a solution where all coefficients $p_{\Delta,l}$ are non-negative would clearly be impossible. We refer to this simple reasoning as the "positivity argument."

One can imagine more general criteria using different differential operators, and applying them at different points. In [7], we found it convenient to apply differential operators precisely at the self-dual point $z = 1/2$, $X = Y = 0$. One can show that the F functions are even with respect to this point both in the X and Y directions:

$$F(X, Y) = F(X, -Y) = F(-X, Y).$$

Thus, all odd-order derivatives vanish, and a sufficiently general differential operator ("linear functional") takes the form:

$$\Lambda[F] = \sum_{\substack{m,n \text{ even} \\ 2 \leq m+n \leq N}} \lambda_{m,n} \partial_X^m \partial_Y^n F|_{X=Y=0}, \quad (3.1)$$

where N is some fixed finite number, and $\lambda_{m,n}$ are fixed real coefficients.[5] Notice the exclusion of the constant term $m = n = 0$, in order to have $\Lambda[1] = 0$.

Assume that for certain fixed d and $\Delta_{\min}$, we manage to find a linear functional of this form such that ("positivity property")

$$\Lambda[F_{d,\Delta,l}] \geq 0 \quad \text{for all } \Delta \geq \Delta_{\min}(l = 0)$$
$$\text{and for all } \Delta \geq l + 2(l = 2, 4, 6 \ldots). \quad (3.2)$$

Moreover, assume that all but a finite number of these inequalities are actually strict: $\Lambda[F] > 0$. Then the sum rule cannot be satisfied, and such a spectrum, corresponding to a putative OPE (1.2), is ruled out.

The proof uses the above "positivity argument." Since $\Lambda[1] = 0$, the positivity property implies that only those primaries for which $\Lambda[F] = 0$ would be allowed to appear in the RHS of the sum rule with nonzero coefficients. By assumption, there are at most a finite number of such primaries. However, as noted in Sec. II B, finitely many terms can never satisfy the sum rule globally, because of the behavior near $z = 0, 1$. Q.E.D.

While the above formal reasoning is quite sufficient to understand our results, in [7] the sum rule was also given an alternative interpretation in terms of convex geometry. In this more visual picture, linear combinations of F functions with arbitrary positive coefficients form a *convex cone* in the space of two-variable functions. One can consider the full function space or its finite-dimensional subspace corresponding to Taylor-expanding up to order N. Positivity property (3.2) means that there is a hyperplane separating the function 1 from the convex cone. Thus it implies that the sum rule cannot be satisfied. The converse is "almost true," modulo questions of convergence.

Clearly, the language of linear functionals provides an equivalent, dual formulation of the problem. This formu-

[5] In [7], we analytically continued to the Minkowski space by Wick-rotating $Y \to iT$. In this picture z and $\bar{z}$ are both real and independent, and conformal blocks are real regular functions in the region $0 < z, \bar{z} < 1$. For our purposes Minkowski and Euclidean pictures are exactly equivalent. In particular, derivatives of F functions in Y and T are trivially proportional to each other.

lation is also especially convenient from the point of view of checking our results independently. It's not so important *how* we find the functionals. As long as we publish the functional coefficients $\lambda_{m,n}$, anyone can verify that the inequalities (3.2) are satisfied.

IV. RESULTS, DISCUSSION, AND 2D ANALOGUE

As discussed in Sec. I, we are interested in computing an upper bound (1.3) for the dimension $\Delta_{\min}$ of the leading scalar in the OPE $\phi_d \times \phi_d$, universal for all unitary 4D CFTs. In [7], we have computed such a bound in the interval $1 \le d \le 1.3$, using the sum rule of Sec. II B truncated to the $N = 6$ derivative order. That bound is reproduced in Fig. 3.

We now present the results of our latest study, obtained for larger values of N. These results[6] are plotted in Fig. 6 as a collection of curves $f_N(d)$, $N = 6 \ldots 18$, where the index N denotes the number of derivatives used to obtain the bound. The bound naturally gets stronger as N increases (see below), and thus the lowest curve $f_{18}(d)$ is the strongest bound to date. In the considered interval $1 \le d \le 1.7$ this bound is well approximated (within 0.5%) by

$$f_{18}(d) \simeq 2 + 0.7\gamma^{1/2} + 2.1\gamma + 0.43\gamma^{3/2}, \qquad \gamma = d - 1. \tag{4.1}$$

To obtain the bounds of Fig. 6, we used the positivity argument from [7], as reviewed in Sec. III. Namely, for points lying on the curves $\Delta_{\min} = f_N(d)$ we are able to find a linear functional of the form (3.1) satisfying the positivity property (3.2).[7] The numerical procedure that we use to find these "positive functionals" is described in some detail in Appendix A.

Several comments are in order here.

(1) We have actually computed the bound only for a discrete number of d values, shown as points in Fig. 6. The tables of these computed values are given in Appendix B. Behavior for $d \to 1$ can be better appreciated from the logarithmic-scale plot in Fig. 7. We do not see any significant indication which could suggest that the curves $f_N(d)$ do not interpolate smoothly in between the computed points. Small irregularities in the slope are however visible at several points in Figs. 6 and 7. These irregularities are understood; they originate from the necessity to *discretize* the infinite system of inequalities (3.2): see Appendix A for a discussion. In our computations the discretization step was chosen so that these irregularities are typically much smaller than the improvement of the bound that one gets for $N \to N + 2$.

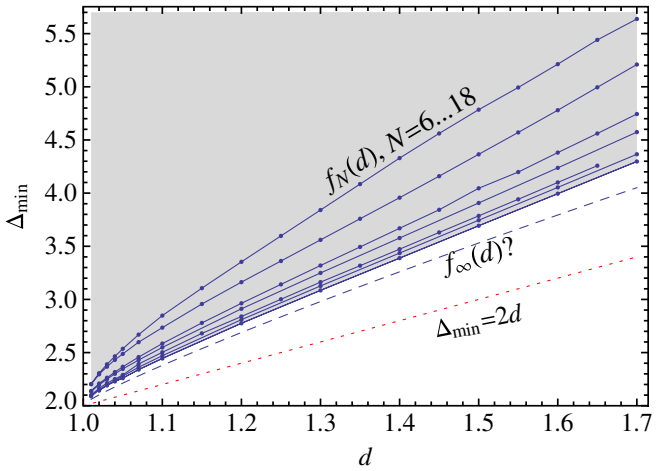

FIG. 6 (color online). Our main results. The solid curves are the bounds $f_N(d)$, $N = 6 \ldots 18$. The bounds get stronger as N increases, thus $N = 6$ is the weakest bound (highest curve), and $N = 18$ is the current best bound (lowest curve). The shaded region is thus excluded. The dashed curve $f_\infty(d)$ is an approximation to the best-possible bound, obtained by extrapolating $N \to \infty$. The dotted line $\Delta_{\min} = 2d$ is realized in a family of "generalized free scalar" CFTs, and is compatible with our bounds.

(2) For each N the bound $f_N(d)$ is near optimal, in the sense that no positive functional involving derivatives up to order N exists for

$$\Delta_{\min} - 2 < (1 - \varepsilon)[f_N(d) - 2].$$

We estimate $\varepsilon \simeq 1\%$ from the analysis of residuals in the fit of $f_N(d)$ by a smooth curve like in (4.1). On the other hand, by increasing N we are allowing more general functionals, and thus the bound $f_N(d)$ can and does get stronger. This is intuitively clear since for larger N the Taylor-expanded sum rule includes more and more constraints.

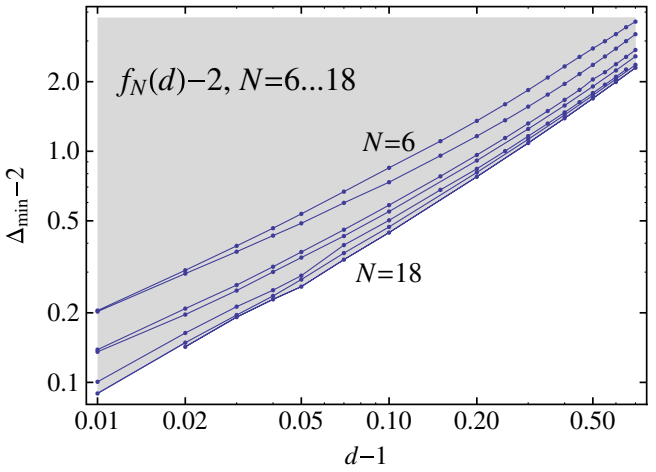

FIG. 7 (color online). Same as Fig. 6 but with anomalous dimensions $d - 1$, $\Delta - 2$ in logarithmic scale. The shaded region is excluded.

[6] See Appendix B for the same results in tabular form.

[7] Thus actually the bound is strict: $\Delta_{\min} < f_N(d)$, except at $d = 1$.

Compared to the results of [7], the bound on the anomalous dimension $\Delta_{\min} - 2$ is improved by $\sim 30 \div 50\%$ in the range $1 \leq d \leq 1.7$ that we explored.

(3) We have pushed our analysis to such large values of N in the hope of seeing that the bound saturates as $N \to \infty$. Indeed, we do observe signs of convergence in Figs. 6 and 7, especially at $d \gtrsim 1.1$. In fact, we have observed that the bounds $f_N(d)$ starting from $N = 8$ follow rather closely the asymptotic behavior

$$f_N(d) \simeq f_\infty(d) + \frac{c(d)}{N^2}, \qquad (1 \leq d \leq 1.7).$$

An approximation to the optimal bound $f_\infty(d)$ can thus be found by performing for each d a fit to this formula. This approximation is shown by a dashed line in Fig. 6. From this rough analysis we conclude that the optimal bound on the anomalous dimension $\Delta_{\min} - 2$ is probably within $\sim 10\%$ from our current bound.

(4) We have $f_N(d) \to 2$ continuously as $d \to 1$. The point $d = 1$, $\Delta_{\min} = 2$ corresponds to the free scalar theory.

We do not know of any unitary CFTs that saturate our bound at $d > 1$; see the discussion in Sec. 6 of [7]. We know however a family of unitary 4D CFTs in which $\Delta_{\min} = 2d$ and which are consistent with our bound (the red dotted line in Fig. 6). This "generalized free scalar" theory is defined for a fixed d by specifying the two-point function

$$\langle \phi(x)\phi(0)\rangle = |x|^{-2d},$$

and defining all other correlators of ϕ via Wick's theorem. This simple procedure gives a well-defined CFT, unitary as long as $d \geq 1$, which can be described by a nonlocal action

$$S \propto \int d^4x \phi(\partial^2)^d \phi.$$

The full operator content of this theory can be recovered by studying the OPE $\phi \times \phi$. In particular, the leading scalar in this OPE has dimension $2d$.[8]

A. 2D analogue

Although our main interest is in the 4D CFTs, our methods allow a parallel treatment of the 2D case. The main characteristics of the 2D situation were described in Sec. 6.1 of [7], here will briefly review them.

(1) At present we can only take advantage of the finite-dimensional $SL(2, \mathbb{C})$ symmetry and not of the full Virasoro algebra of the 2D CFTs. In particular, our results are independent of the 2D central charge c.

(2) The unitarity bounds for $SL(2, \mathbb{C})$ primaries[9] in 2D have the form

$$\Delta \geq l, \qquad l = 0, 1, 2 \ldots,$$

where l is the Lorentz spin.

(3) The $SL(2, \mathbb{C})$ conformal blocks in 2D are known explicitly [10]:

$$g_{\Delta,l}(u, v) = \frac{(-)^l}{2^l}[f_{\Delta+l}(z)f_{\Delta-l}(\bar{z}) + (z \leftrightarrow \bar{z})]. \tag{4.2}$$

Using the unitarity bounds, the known conformal blocks, and the sum rule (2.8), valid in any dimension, we can try to answer the same question as in 4D. Namely, for a $SL(2, \mathbb{C})$ scalar primary ϕ of dimension d, what is an upper bound on the dimension $\Delta_{\min}$ of the first scalar operator appearing in the OPE $\phi \times \phi$? I.e. we want a 2D analogue of the bound (1.3). Since the free scalar is dimensionless in 2D, the region of interest is $d > 0$.

Figure 8 summarizes our current knowledge of this bound[10]:

(i) The dotted line is the old $N = 2$ bound presented in [7]. The solid line is the $N = 12$ improved bound obtained by us.[11] A numerical fit to this bound is given by

$$f_{12}^{(2D)}(d) \simeq \begin{cases} 4.3d + 8d^2 - 87d^3 + 2300d^4, & d \lesssim 0.122, \\ 0.64 + 2.87d, & d \gtrsim 0.122. \end{cases}$$

Clearly, the improvement compared to [7] is significant.

It is interesting to note that in 2D we have observed a much faster convergence for increasing N than in 4D. In fact, already with $N = 6$ it is possible to obtain a bound rather close to the one shown in Fig. 8, although with a slightly rounded "knee." We have also computed several points for $N = 16$ and have not seen much improvement.

(ii) The dashed line and scattered crosses correspond to various OPEs realized in explicit examples of exactly solvable unitary 2D CFTs (minimal models and the free scalar theory); see [7]. They all respect our bound.

It is instructive to compare this plot with its 4D counterpart, Fig. 6. While we do not know of any CFTs

[8]This theory can also be realized holographically by considering a free scalar field of a particular d-dependent mass in the AdS geometry and taking the limit in which 5D gravity is decoupled. We are grateful to Kyriakos Papadodimas for discussions about the generalized free scalar CFT.

[9]Known as quasiprimaries in 2D CFT literature.

[10]See Appendix B for the results in tabular form.

[11]We are grateful to Erik Tonni for providing us with the large Δ, l asymptotics of the 2D conformal block expansion coefficients, necessary to obtain this bound.

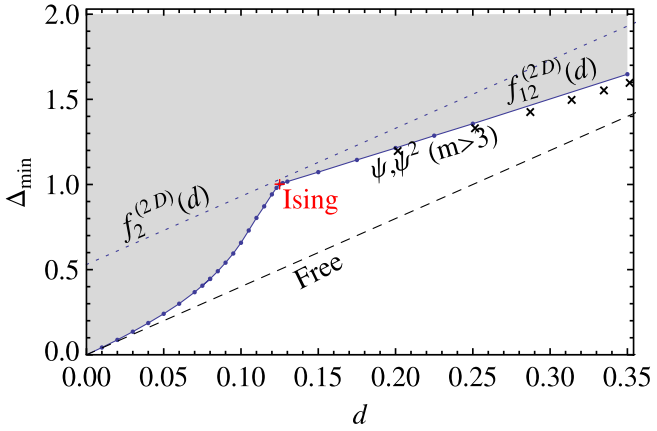

FIG. 8 (color online). See the text for an explanation. The + cross denotes the position of the Ising model, the × crosses marked ψ, ψ^2 correspond to the OPEs realized in the higher minimal models, as in Fig. 15 of [7]. The shaded region is excluded.

saturating the 4D bound, the 2D unitary minimal models $\mathcal{M}(m, m+1)$, $m = 3, 4, \ldots$, contain the OPEs

$$\psi \times \psi = 1 + \psi^2 + \ldots, \qquad \Delta_\psi = \frac{1}{2} - \frac{3}{2(m+1)},$$
$$\Delta_{\psi^2} = 2 - \frac{4}{m+1}, \tag{4.3}$$

which come quite close to saturating the 2D bound.

More precisely, our 2D bound starts at (0, 0) tangentially to the line $\Delta = 4d$ realized in the free scalar theory, then grows monotonically and passes remarkably closely above the Ising model point $(\Delta_\sigma, \Delta_\varepsilon) = (1/8, 1)$. After a knee at the Ising point, the bound continues to grow linearly, passing in the vicinity of the higher minimal model points (4.3).

It is curious to note that if we did not know beforehand about the Ising model, we could have conjectured its field dimensions and the basic OPE $\sigma \times \sigma = 1 + \varepsilon$ based on the singular behavior of the 2D bound at $d = 1/8$.

On the other hand, nothing special happens with the 2D bound at the higher minimal model points, it just interpolates linearly in between.[12] Most likely, this does not mean that there exist other unitary CFTs with intermediate operator dimensions. Rather, this behavior suggests that the single conformal bootstrap equation used to derive the bound is not powerful enough to fully constrain a CFT.

In comparison, it is a bit unfortunate that the 4D bound does not exhibit any singular points which would immediately stand out as CFT candidates. Nevertheless, if we assume that the shape of the 4D bound is a result of an interpolation between existing CFTs (as it is the case in 2D), we may conjecture that the upward convex behavior of the functions $f_N(d)$ in Fig. 6 is due to the presence of a family of points satisfying the sum rule that can correspond to exact CFTs. This observation, though speculative, shows how the presented method can provide a guideline in the study of 4D CFTs.

[12]The straight line fitting the bound would cross the dashed Free theory line just above $d = 0.5$, which is the accumulation point of the minimal models $\mathcal{M}(m, m+1)$. For larger values of d we expect that the bound modifies its slope and eventually asymptotes to the Free line.

V. FUTURE RESEARCH DIRECTIONS

The results of this paper and of [7] open up many interesting research directions, which we would like to list here.

First, there are several important problems in 4D conformal field theory which can be analyzed by our method and its simple modifications. For example:

(1) One should be able to derive a generalization of our bounds in the situation when the CFT has a global symmetry, and we are interested in the lowest dimension *singlet* appearing in the OPE. This is going to have phenomenological implications by constraining the so-called conformal technicolor scenarios of electro-weak symmetry breaking [11]. This connection was extensively discussed in [7].

(2) One should be able to derive model-independent bounds on the size of OPE coefficients. This is going to be relevant for discussions of "unparticle self-interactions" [12], in the context of unparticle physics scenarios [13].

Second, the method can also be used in 2D conformal field theory, as was already demonstrated in Sec. IV A. The main interest here lies in potential applications to string theory. We will now briefly describe two such applications.

Physical states of (super)string theory are in 1-1 correspondence with Virasoro primary operators of a 2D CFT living on the string world sheet. The mass of a string state (in string units) is related to the corresponding primary operator dimension Δ via

$$m^2 = \Delta - 2.$$

We are considering closed string theory for concreteness. When strings propagate in flat space, the CFT is solvable and the full spectrum of operator dimensions is known. Realistic string constructions require compactifications of extra dimensions. In some examples, such as toroidal compactifications, the CFT is still solvable. In others, such as superstring compactifications on a generic Calabi-Yau three-fold, the CFT cannot be solved exactly. All what is generally known is the spectrum of the massless states, which can be obtained in the supergravity approximation. Of course we expect the massive string states to be always present, but just how heavy can they be? We know from the experience with toroidal compactifications that it is impossible to completely decouple the massive states: as the compactification radius $R \to 0$, the Kaluza-Klein states

become more massive, but the winding modes come down. Clearly, massive string states are crucial for the consistency of the theory. What exactly are they doing? A partial answer may be that without their presence, four-point functions of the massless state vertex operators would not be crossing-symmetric. If this intuition is right, it could be used to obtain model-independent bounds on the lightest massive states in string compactifications, generalizing the well-known bounds valid for toroidal compactifications. A similar in spirit general prediction of string gravity, although in a different context and by using different methods, was obtained recently in [14].

When working towards results of this kind, it may be necessary to generalize our methods so that the information about the 2D CFT central charge, which is fixed in string theory, can be taken into account. In practice, one needs an efficient method to evaluate the full Virasoro conformal blocks. While no closed-form expression as simple as Eq. (4.2) is known, Zamolodchikov's expansion (see [6]) can probably be applied.

Finally, as mentioned above in the 4D context, it should be possible to derive model-independent bounds on the OPE coefficients. Such results must be accessible via a simple modification of our method, in particular, the full Virasoro conformal blocks are not needed here. One can then apply such bounds to the dimension 2 operators corresponding to the massless string states (in an arbitrary compactification). Via the usual dictionary, this would then translate into general bounds on the tree-level coupling constants in the low-energy string effective actions.

VI. SUMMARY

Prime principles of conformal field theory, such as unitarity, OPE, and conformal block decomposition, imply the existence of an upper bound $f(d)$ on the dimension $\Delta_{\min}$ of the leading scalar operator in the OPE $\phi \times \phi$, which depends only on ϕ's dimension d.

Moreover, there is an efficient method which allows numerical determination of $f(d)$ with arbitrary desired accuracy. The method is based on the *sum rule*, a function-space identity satisfied by the conformal block decomposition of the four-point function $\langle \phi\phi\phi\phi \rangle$, which follows from the crossing symmetry constraints. In practical application of the method the sum rule is Taylor-expanded: replaced by finitely many equations for the derivatives up to a certain order N. The bound $f(d)$ improves monotonically as more and more derivatives are included. In [7], where the above paradigm was first developed, we numerically computed the bound for $N = 6$.

The present paper extended the study of [7] to higher N. The goals were to improve the bound, and perhaps to approach the best-possible bound in case a convergence of the bound is observed.

Our analysis went up to $N = 18$ (see Fig. 6) and we have achieved both goals. First, in the range $1 \leq d \leq 1.7$ that we explored, the bound on the anomalous dimension $\Delta_{\min} - 2$ is improved by $30 \div 50\%$ compared to the results of [7]. Second, we do observe signs of convergence of the bound. We believe that our current results are close (within $\sim 10\%$) to the best ones achievable with this method.

The results of this paper and of [7] suggest several interesting research directions, connected with phenomenology and, via the 2D analogue of our method, with string theory (see Section V).

ACKNOWLEDGMENTS

We are grateful to J. Maldacena, A. M. Polyakov, and N. Seiberg for discussions of possible applications of our methods in string theory, to A. M. Polyakov for bringing the subtleties of the analytic structure of the conformal blocks to our attention, and to K. Papadodimas for discussions of the generalized free scalar theory. We are especially grateful to our collaborators R. Rattazzi and E. Tonni for many discussions related to this project, and, in particular, to E. Tonni for providing us with the large Δ, l asymptotics of the 2D conformal block expansion coefficients. This work is partially supported by the EU under RTN Contract No. MRTN-CT-2004-503369, by MIUR under Contract No. PRIN-2006022501, and by the Swiss National Science Foundation under Contract No. 200021-116372. V. R. thanks Laboratoire de Physique Théorique de l'Ecole Normale Supérieure for hospitality.

APPENDIX A: DETAILS ABOUT NUMERICAL ALGORITHMS

We now discuss in more detail the issues introduced in Sec. III, namely, how we can find in practice a linear functional $\Lambda[F]$ of the form (3.1) satisfying the positivity property (3.2). We will first describe the general procedure and how it can implemented in a computer code, and then mention possible algorithmic improvements and shortcuts that we found useful in our analysis.

Given the complexity of the functions $F_{d,\Delta,l}$, the search for a positive functional is too hard a task to be attacked analytically. As already mentioned, we reduce the complexity of the problem by looking for a functional which is a linear combination of derivatives up to a given order N. The derivative are taken with respect to (w.r.t.) the self-dual point $X = Y = 0$, since the sum rule is expected to converge fastest around this point and, in addition, the functions $F_{d,\Delta,l}(X, Y)$ are even in both arguments. The choice of the functional (3.1) simplifies our task enormously since we can now work in a finite-dimensional space, and the only information concerning $F_{d,\Delta,l}$ that we need are their derivatives up to a certain order. Put another way, the F functions are now considered as elements not of a function space but of a finite-dimensional vector space $\mathbb{R}^s$, $s = N(N + 6)/8$.

The sum rule (2.8) in this picture represents a constraint on these vectors that, in any CFT, must sum to zero. This

interpretation is discussed in detail in [7]. Here we adopt an equivalent point of view in terms of the dual space of linear functionals defined on $\mathbb{R}^s$ since we find this prospective closer to the method used to obtain numerically $\Lambda[F]$.

Let us fix the notation. We define the s-dimensional vector of Taylor coefficients:

$$\mathcal{F}_0[d,\delta,l] \equiv \left\{\frac{1}{m!n!}F^{(m,n)}_{d,\Delta,l} | m,n \text{ even}, \ 2 \le m+n \le N\right\},$$
$$F^{(m,n)}_{d,\Delta,l} \equiv \partial^m_X \partial^n_Y F_{d,\Delta,l}|_{X=Y=0}, \qquad \delta \equiv \Delta - l - 2, \tag{A1}$$

and the same vector normalized to the unit length:

$$\mathcal{F}[d,\delta,l] \equiv \frac{\mathcal{F}_0}{\|\mathcal{F}_0\|}, \tag{A2}$$

where the norm $\|\mathcal{F}_0\|$ is the usual Euclidean length of the vector $\mathcal{F}_0$.

We form the vector $\mathcal{F}_0$ out of the Taylor coefficients of the function $F_{d,\Delta,,l}$ rather then of its derivatives, because this way all elements turn out to have approximately the same order of magnitude, which is preferable in the subsequent numerical computation. The definition of the normalized vector $\mathcal{F}$ serves the same purpose. Indeed, as explained in the following, our numerical analysis consist in finding a solution of a system of linear inequalities where the coefficient are given by the elements of $\mathcal{F}[d,\delta,l]$. The solution is more accurate and easier to extract if all the coefficient are of the same order of magnitude. Since the existence of the functional Λ is not affected by these rescalings, we opted for the definition (A1) and (A2).

According to the positivity property we look for a functional which is strictly positive on all but finitely many vectors $\mathcal{F}[d,\delta,l]$. Let us fix the dimension d of the scalar ϕ_d. Then each pair Δ, l identifies the semispace of $(\mathbb{R}^s)^*$ of the functionals positive definite on the vectors $\mathcal{F}[d,\delta,l]$; let us call this open sets $U_{d,\Delta,l}$. With this notation the positivity property (3.2) can be restated in the following way: *If for fixed d and $\Delta_{\min}$*

$$\bigcap_{\substack{\Delta \ge \Delta_{\min}, l=0 \\ \Delta \ge l+2, l=2,4,\ldots}} U_{d,\Delta,l} \neq \varnothing, \tag{A3}$$

then the sum rule cannot be satisfied. The issue is thus to be able to check whether the intersection (A3) is nonempty, and to compute the smallest $\Delta_{\min}$ for which this is the case.

Clearly it is neither possible nor needed to check all the values of Δ as required by the condition (A3). We can indeed consider only a finite number of them and check if they admit the existence of a functional or not. This can be achieved with a double simplification. First, we consider values of Δ and l only up to a given maximum value (''truncation''), and second, we discretize the kept range of Δ (''discretization''). The truncation does not produce a loss of information since we take into account the large Δ and l contributions using the asymptotic expressions computed in Appendix D of [7]. The discretization step requires special care; see below.

We used MATHEMATICA 7 to perform the computations. The algorithm to extract the smallest value of $\Delta_{\min}$ proceeds in several steps:

(1) Setting up an efficient procedure to compute vectors $\mathcal{F}[d,\delta,l]$.

(2) Selection of the l's and δ's to be used in checking the positivity property (A3). For concreteness we report here the range of l, δ that we were including[13]:

$$2 \le l \le l_{\max} = 50: \quad 0 \le \delta \le 200,$$
$$l = 0: \quad \delta_{\min} \equiv \Delta_{\min} - 2 \le \delta \le 200. \tag{A4}$$

For each l the range of δ was discretized, and a discrete set of points was chosen, called Γ_l below. The derivatives of the F functions approach zero as $\delta \to \infty$ and reach the asymptotic behavior for sufficiently large values. We take a finer discretization where the function are significantly varying while we can allow to increase the step in the asymptotic region. More details are given below.

(3) Reduction to a *Linear Programming* problem. With only a finite number of equations to check, the determination of the intersection of the $U_{d,\Delta,l}$ becomes a standard problem of *Linear Programming* which can be solved in finite amount of time. Hence we look for a solution of the linear system of inequalities

$$\Lambda[\mathcal{F}[d,\delta,l]] \equiv \sum \tilde{\lambda}_{m,n}\mathcal{F}_{m,n} \ge 0,$$
$$\delta \in \Gamma_l, \qquad l = 0 \ldots l_{\max}. \tag{A5}$$

Clearly, the coefficients $\tilde{\lambda}_{m,n}$ are related to those appearing in (3.1) by a trivial rescaling depending on m, n:

$$\tilde{\lambda}_{m,n} = m!n!\lambda_{m,n}$$

Further, the asymptotic behavior of the F functions (see below) tells us that for large δ the inequality is dominated by the $(N,0)$ derivative

$$\Lambda[F_{d,\Delta,l}] \to \tilde{\lambda}_{N,0}F^{(N,0)}_{d,\Delta,l} \qquad (\delta \gg l \gg 1), \tag{A6}$$

hence $\tilde{\lambda}_{N,0}$ needs to be positive. By an overall rescaling of Λ we can always achieve

$$\tilde{\lambda}_{N,0} = 1, \tag{A7}$$

which we choose as a normalization condition.

[13] In some cases $2 < l < 200$ was needed to obtain a functional which would later pass the positivity check on the nonincluded values of l; see below.

(4) Extraction of the smallest $\Delta_{\min}$ for which a positive functional exists. We begin by selecting two points $\delta_{\min} = \delta_1$ and $\delta_{\min} = \delta_2 > \delta_1$ [see (A4)] such that we know *a priori* that in the first case a positive functional does not exists, while in the second case it does.[14] Starting from these values we apply the bisection method to determine the critical $\delta_{\min}$ up to the desired precision: we test if a functional exists for $\delta_{\min} = (\delta_2 + \delta_1)/2$ and we increase or decrease the extremes of the interval $[\delta_1, \delta_2]$ depending on the outcome. The procedure we follow is such that in the end the critical $\delta_{\min}$ is contained in an interval of relative width 10^{-3}, i.e. we terminate if $\delta_2 - \delta_1 \leq 10^{-3}\delta_1$. The plots and the tables presented in this work correspond to the upper end δ_2 of the final interval, i.e. to the end for which we have found a functional.

Let us now come back to the point 1. Although computation of the derivatives can be carried on by brute force Taylor-expanding the F functions, we can save time decomposing the computation in various blocks. From Eq. (2.8) we see the rather simple dependence on the parameter d, which translates in a polynomial dependence once the function is Taylor-expanded in X and Y. We therefore separately computed the dependence on d once and for all as a matrix $M(d)_{mn|ij}$. To compute Taylor coefficients of F functions, this matrix is contracted with two vectors containing one-dimensional Taylor coefficients of the function $k_\beta(x)$; see (2.4). The latter derivatives are precomputed for several values of β with a fine step and stored. For definiteness we report the interval we used

$$0 \leq \beta \leq 10^2, \qquad \text{step: } 10^{-3}. \tag{A8}$$

For larger β we made use of the analytic expression of the asymptotics instead of computing the derivatives numerically (see below).

Finally let us discuss the choice of the discretization and the truncation in Δ and l. This step is of fundamental importance in order to reduce the time needed to perform the computation.

In Appendix D of [7] it is shown that for large values of δ and l the functions $F_{d,\Delta,l}$ approach an asymptotic behavior. We have checked that outside the range of values (A4) we can safely use the approximate expression

$$F^{(m,n)}_{d,\Delta,l} \sim \text{const}(2\sqrt{2})^{m+n+2}\frac{(l+\delta)^{m+1}l^{n+1}}{(m+1)(n+1)}.$$

For large l, δ the vector $\mathcal{F}[d, \delta, l]$ is dominated by the components where $m + n$ assumes the highest allowed value N. Hence we can take into account this large l, δ behavior imposing additional constraints:

$$\Lambda[\mathcal{F}_\theta] \geq 0,$$
$$\mathcal{F}_\theta = \begin{cases} \frac{(\cos\theta+\sin\theta)^{m+1}\cos\theta^{n+1}}{(m+1)(n+1)} & \text{if } m+n=N \\ 0 & \text{otherwise} \end{cases},$$
$$\tan\theta \equiv \frac{\delta}{l},$$

where we have dropped irrelevant positive constants not depending on m, n.

Now comes the discretization: in the range of values (A4), as well as in the interval $\theta \in [0, \pi/2]$, we can allow to take only a discrete, finite number of points. For θ we take a fixed small step. However, for δ we try to concentrate the points in the region where the unit vector $\mathcal{F}[d, \delta, l]$ is significantly varying. A measure of this is given by the norm of its derivative w.r.t. δ[15]:

$$\mathcal{N} = \left\| \frac{\partial}{\partial\delta}\mathcal{F}[d, \delta, l] \right\|.$$

We discretize by taking the spacing between two consecutive values of δ equal $c/\mathcal{N}$, where c is a small fixed number ($c = 0.02 \div 0.05$ was typically taken in our work). Clearly when the unit vector is slowly varying the discretization step is large, while it is refined where it is changing rapidly, and where presumably more information is encoded. Typically we get about a hundred δ values for each l, but only a few dozen of those above $\delta > 50$.

The sets Γ_l, one for each l, of values of δ obtained in this way are the ones referred to at point 2 above. In constructing the linear system that we use at point 3 we consider additional intermediate points between two subsequent δ's. In order to understand why we do this, let us assume that we have found a functional Λ which is positive for all the values of δ contained in Γ_l. Since we considered a discrete set of values, it may and actually does happen that for intermediate values of δ (which were not included in Γ_l) the functional becomes slightly negative. In [7] this issue was solved looking for solution of the form $\Lambda[F_{d,\Delta,l}] > \varepsilon$, so that for intermediate values this condition could be violated but the positivity was safe. In the current work we found it more convenient to build the linear system in the following way:

(i) for each $\delta \in \Gamma_l = \{\delta_1, \ldots, \delta_i, \delta_{i+1}, \ldots\}$ we evaluate the vector $\mathcal{F}[d, \delta, l]$.

(ii) for any two consecutive points δ_i, δ_{i+1}, we consider the first-order Taylor expansion of the vector $\mathcal{F}[d, \delta, l]$ around $\delta = \delta_i$ and evaluate it at half-spacing between δ_i and δ_{i+1} (footnote 15):

[14] We can choose these points blindly as $\delta_1 = 0$, $\delta_2 \gg 1$, however prior experience can suggest a choice closer to the final $\delta_{\min}$

[15] In practice the derivative $\partial/\partial\delta$ is evaluated by using the finite-difference approximation.

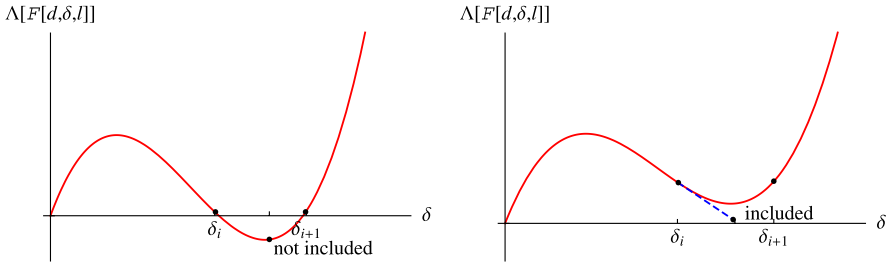

FIG. 9 (color online). Imposing the positivity of the functional on a discrete set of points, it could happen that the intermediate points do not satisfy $\Lambda[\mathcal{F}[d, \delta, l]] \geq 0$ (on the left). However adding the constraint $\Lambda[\mathcal{F}_{1/2}[d, \delta_i, l]] \geq 0$ [see (A9)], we can be sure that the functional is positive on all the neglected points (on the right).

$$\mathcal{F}_{1/2}[d, \delta_i, l] \equiv \mathcal{F}[d, \delta_i, l] + \left(\frac{\delta_{i+1} - \delta_i}{2}\right) \times \frac{\partial}{\partial \delta} \mathcal{F}[d, \delta_i, l] \tag{A9}$$

and we add the constraints $\Lambda[\mathcal{F}_{1/2}] \geq 0$ to the linear system (A5).

These additional constraints become important to keep the functional positive near the δ's for which the inequalities $\Lambda[\mathcal{F}] \geq 0$ are close to saturation, while they are redundant away from those points. Indeed, assume that for some δ_i and δ_{i+1} the functional is exactly vanishing. Then at the intermediate point the functional would be strictly negative, which is not allowed. However, in the presence of the additional constraint $\Lambda[\mathcal{F}_{1/2}] \geq 0$ this cannot happen, since $\Lambda[\mathcal{F}]$ is generically a convex function of δ near the minimum. See Fig. 9 for an illustration. Thus we can be certain that the found functional will be positive also for those δ's which were not included into Γ_l.

This certainty has a price. Namely, the opposite side of the coin is that the added $\mathcal{F}_{1/2}$ constraints are somewhat *stronger* than needed, and the bigger the discretization parameter c, the bigger the difference. As a result, the found critical value of $\Delta_{\min}$ will be somewhat *above* the optimal critical value, corresponding to $c \to 0$. This observation explains why the curves in Figs. 6 and 7 have small irregularities in the slope. These irregularities could be decreased by decreasing the value of c.

Several comments concerning the numerical accuracy are in order. The components of the vector $\mathcal{F}[d, \delta, l]$ have been computed using standard double-precision arithmetic (16 digits). As a consequence all the numerical results must be rounded to this precision. In particular, quantities smaller that 10^{-16} are considered zero.

In addition, the built-in MATHEMATICA 7 function `LinearProgramming`, which we used, has an undocumented `Tolerance` parameter. Most of the computations were done with `Tolerance` equal 10^{-6} (default value). However for $N = 16$ and $N = 18$, and for $d < 1.1$, we found that `LinearProgramming` terminates prematurely, concluding that no positive linear functional exists, even for some values of $\delta_{\min}$ for which a positive functional for smaller N was in fact found. The problem disappeared once we set `Tolerance` to a lower value (10^{-12}). In our opinion, `Tolerance` is probably the so-called *pivot tolerance*, the minimal absolute value of a number in the pivot column of the simplex method to be considered nonzero. Recall that a nonzero (actually negative) pivot element is necessary in each step of the simplex method [15]. This interpretation explains why the above problem could occur, and why it could be overcome by lowering `Tolerance`.

As described above, our numerical procedure has been designed to be robust with respect to the effects of truncation and discretization. In addition, for each d, we have tested the last found functional (i.e. for $\delta_{\min}$ at the upper end δ_2 of the final interval $[\delta_1, \delta_2]$) on the much bigger set of δ, l:

$$\begin{aligned} &2 \leq l \leq 500, \qquad 0 \leq \delta \leq 500, \qquad \text{step} = 0.1, \\ &l = 0, \qquad \delta_{\min} \leq \delta \leq 500, \qquad \text{step} = 0.1, \end{aligned} \tag{A10}$$

and found that indeed $\Lambda[\mathcal{F}] \geq 0$, within the declared 10^{-16} accuracy.

Finally, we have checked that in all cases the found functionals Λ are such that the inequality $\Lambda[\mathcal{F}] \geq 0$ is in fact strict: $\Lambda[\mathcal{F}] > 0$, for all but finitely many values of δ and l. Thus they satisfy the requirements stated in Sec. III.

APPENDIX B: TABLES

Table I contains the sequence of 4D bounds $f_N(d)$, $N = 6 \ldots 18$, for a discrete set of points in the interval $1 < d \leq 1.7$. Table II contains the 2D bound $f_{12}^{(2D)}(d)$ for a discrete set of points in the interval $0 < d \leq 0.35$. Figures 6–8 are based on these tables.

A text file with the unrounded versions of Tables I and II and the functionals used to derive these bounds can be downloaded [16]. The MATHEMATICA codes can be obtained from the authors upon request.

TABLE I. 4D results. The table contains anomalous dimensions, i.e. $d-1$ and $f_N(d)-2$ are given. A zero entry means that the bound for this d and N has not been computed.

				$f_N(d)-2$			
$d-1$	$N=6$	$N=8$	$N=10$	$N=12$	$N=14$	$N=16$	$N=18$
0.01	0.2045	0.2025	0.1385	0.1356	0.1006	0.089 55	0
0.02	0.3055	0.2956	0.2086	0.1965	0.1636	0.1485	0.1425
0.03	0.3895	0.3676	0.2636	0.2496	0.2126	0.1956	0.1916
0.04	0.4646	0.4315	0.3165	0.3006	0.2506	0.2366	0.2286
0.05	0.5358	0.4878	0.3665	0.3467	0.2896	0.2786	0.2596
0.07	0.6688	0.598	0.4576	0.4296	0.3927	0.3627	0.3397
0.1	0.848	0.7348	0.5847	0.5486	0.5026	0.4705	0.4448
0.15	1.106	0.957	0.7789	0	0.6807	0	0
0.2	1.354	1.163	0.9635	0.9118	0.8396	0.8098	0.7757
0.25	1.597	1.362	1.142	0	1.002	0	0
0.3	1.841	1.56	1.319	1.249	1.163	1.127	1.085
0.35	2.085	1.759	1.494	0	1.317	0	0
0.4	2.329	1.957	1.669	1.578	1.473	1.436	1.389
0.45	2.561	2.159	1.843	0	1.63	0	0
0.5	2.785	2.365	2.046	1.907	1.786	1.745	1.693
0.55	2.994	2.571	2.198	0	1.942	0	0
0.6	3.213	2.78	2.381	2.238	2.1	2.054	1.995
0.65	3.441	2.995	2.561	0	2.258	0	0
0.7	3.638	3.21	2.744	2.574	0	2.366	2.297

TABLE II. 2D results.

d	$f_{12}^{(2D)}(d)$
0.01	0.042 54
0.02	0.087 52
0.03	0.1356
0.04	0.1865
0.05	0.2406
0.06	0.2998
0.07	0.3676
0.08	0.4455
0.075	0.4055
0.08	0.4456
0.085	0.4907
0.09	0.5408
0.095	0.5947
0.1	0.6577
0.105	0.73
0.11	0.8037
0.115	0.8716
0.12	0.9418
0.123	0.9803
0.125	1.001
0.127	1.008
0.13	1.017
0.15	1.073
0.2	1.214
0.25	1.357
0.35	1.647

[1] A. A. Belavin and A. A. Migdal, JETP Lett. **19**, 181 (1974) [Pis'ma Zh. Eksp. Teor. Fiz. **19**, 317 (1974)]; T. Banks and A. Zaks, Nucl. Phys. **B196**, 189 (1982).

[2] N. Seiberg, Nucl. Phys. **B435**, 129 (1995).

[3] Y. Iwasaki, K. Kanaya, S. Kaya, S. Sakai, and T. Yoshie, Phys. Rev. D **69**, 014507 (2004); T. Appelquist, G. T. Fleming, and E. T. Neil, Phys. Rev. Lett. **100**, 171607 (2008); arXiv:0901.3766; A. Deuzeman, M. P. Lombardo, and E. Pallante, Phys. Lett. B **670**, 41 (2008); arXiv:0904.4662.

[4] G. Mack, Commun. Math. Phys. **55**, 1 (1977).

[5] A. M. Polyakov, Zh. Eksp. Teor. Fiz. **66**, 23 (1974); A. A. Belavin, A. M. Polyakov, and A. B. Zamolodchikov, Nucl. Phys. **B241**, 333 (1984).

[6] A. B. Zamolodchikov and A. B. Zamolodchikov, Report No. ITEP-90-31; Nucl. Phys. **B477**, 577 (1996).

[7] R. Rattazzi, V. S. Rychkov, E. Tonni, and A. Vichi, J. High Energy Phys. 12 (2008) 031.

[8] J. Polchinski, *String Theory: An Introduction to the Bosonic String* (Cambridge University Press, Cambridge, UK, 1998), Vol. 1, p. 402.

[9] G. Mack, Commun. Math. Phys. **53**, 155 (1977).

[10] F. A. Dolan and H. Osborn, Nucl. Phys. **B599**, 459 (2001); Nucl. Phys. **B678**, 491 (2004).

[11] M. A. Luty and T. Okui, J. High Energy Phys. 09 (2006) 070; M. A. Luty, arXiv:0806.1235.

[12] J. L. Feng, A. Rajaraman, and H. Tu, Phys. Rev. D **77**, 075007 (2008); H. Georgi and Y. Kats, arXiv:0904.1962.

[13] H. Georgi, Phys. Rev. Lett. **98**, 221601 (2007).

[14] S. Hellerman, arXiv:0902.2790.

[15] W. H. Press, S. A. Teukolsky, W. T. Vetterling, B. P. Flannery, *Numerical Recipes. The Art of Scientific Computing* (Cambridge University Press, Cambridge, UK, 2007), 3rd ed.

[16] http://www.arxiv.org/e-print/0905.2211.